Structure and Electrical Properties of CdO doped TiO_2 Thin Films Prepared by Pulsed Laser Deposition

Ghuson H. Mohammed[1], Ahmed M. Savory [2], Dunia K.[3], Kadhim A. A[4]

University of Baghdad, Collage of Science, Iraq

Abstract: ***$(TiO_2)_{1-x}(CdO)_x$ thin films have been deposited at different annealing (423 and 523)K with different concentration of CdO of x= (0.0, 0.05, 0.1, 0.15 and 0.2) Wt. % onto glass substrates by pulsed laser deposition technique (PLD) Nd-YAG laser with λ=1064nm, energy=800mJ and number of shots=500. X-ray diffraction (XRD) results reveals that the deposited $(TiO_2)_{1-x}(CdO)_x$ thin films polycrystalline with tetragonal structure and many peaks (110), (101), (111) and (211) were appear The temperatures dependence of the electrical conductivity and the activation energy at temperature ranging from (293-473) K of the as-deposited and films annealed at different annealing temperatures have been studied. The results show that as the film concentration of and conductivity increases, while the activation energy (Ea1, Ea2) decreases. Both, the annealing and composition effects on Hall constant, charge carrier concentration, Hall mobility were investigated. Hall Effect measurements show that all films have n- type charge carriers.***

Keywords: $(TiO_2)_{1-x}(CdO)_x$ Thin Film; structural properties; pulse laser deposition technique; Electrical properties

1. Introduction

Titanium dioxide (TiO_2), a well-known oxide semiconductor material, has been extensively studied owing to its superior physical and chemical properties in photocatalysis [1]. Moreover, TiO_2 is used in solar cells for the production of hydrogen and electric energy gas sensor, white pigment (e.g. in paints and cosmetic products), corrosion-protective coating, an optical coating in ceramics and in electric devices such as varistors. TiO_2 also has many excellent properties such as non-toxicity and long term stability against photo corrosion [2, 3].TiO_2 films have been prepared by many technologies, including magnetron sputtering [4, 5]chemical bath deposition (CBD) method [6, 7], electron-beam evaporation [8], reactive electron beam evaporation [9], sol-gel method [10-14] , and thermal oxidation. Recently there are many applications of laser one of these applications in a thin film preparation field that called pulsed Laser deposition (PLD). With the pulsed laser deposition method, thin films are prepared by the ablation of one or more targets illuminated by a focused pulsed-laser beam. This technique was first used by smith and Turner in 1965 [15] for the preparation of semiconductor and dielectric thin films and was established due to the work of Dijkkamp and coworkers [16] were able to laser-deposit a thin film of YBa_2Cu3O7, a high temperature superconductor material in 1987 which was of superior quality to that of films deposited with alternative techniques.. Cadmium oxide (CdO) has high electrical conductivity and high optical transmittance with a moderate refractive index in the visible region of the solar spectrum. In recent years it has found various applications in transparent electrodes, solar cells, photo transistors, photodiodes, gas sensors, etc. [17, 18]. CdO films are wide, direct band-gap semiconductors with an optical energy gap of about 2.4 eV at room temperature. CdO, with its cubic structure, is also a II-VI n-type semiconductor with donor defects, such as Cd interstitials and oxygen vacancies [19].

2. Experimental Details

Titanium dioxide from Nano shell Company with a purity of 99.99% and cadmium oxide with purity of 99.99% were mixed together at different concentration of x= (0.0, 0.05, 0.1, 0.15, 0.2) Wt. % using agate mortar for 1 hour then the mixture was pressed into pellets of (1.5 cm) in diameter and (0.2 cm) thick, using hydraulic manually type (SPECAC), under pressure of 5 tons. The pellets were sintered in air at temperature of (773 K) for 3 h. The $TiO_{2(1-x)}$ CdO_x films were deposited on glass slides substrates of (10×10 mm). The substrate were cleaned with dilated water using ultrasonic process for 15 minute to deposit the films at room temperature then annealing treatment at (423 and 523) K by furnace under vacuum ($8*10^{-2}$ mbar) were carried out to the films. PLD technique was used to deposit the films under vacuum of (8×10^{-2} mbar) using Nd:YAG with (λ= 1064 nm) SHG Q-switching laser beam at 800 mJ, repetition frequency (6Hz) for 500 laser pulse is incident on the target surface making an angle of 45° with it. The distance between the target and the laser was set to (10 cm), and between the target and the substrate was (1.5 cm). The thickness of $(TiO_2)_{1-x}(CdO)_x$ thin film was measure using optical interferometer method employing He-Ne laser 632 nm with incident angle 45°. This method depends on the interference of the laser beam reflected from thin film surface and then substrate, the films thickness t was determined using the following formula [20]:

$$t = \frac{\lambda}{2} \cdot \frac{\Delta x}{x} \qquad (1)$$

Also, a mask is made from a piece of aluminum foil having (width: 2mm, distance between electrodes 2mm) with the same size of the substrate. These masks are put on glass substrates to deposit the aluminum using (Tungsten W) boat material by using vacuum thermal evaporation technique of type (Balzers-BAE370) under pressure (10^{-5} mbar). Various shapes of masks were used to determine electrical properties

as shown in figure (1)

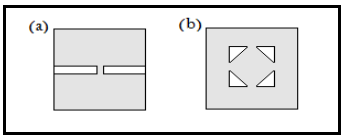

Figure 1: Mask of different shapes and purposes (a) D.C conductivity electrodes (b)Hall effect electrodes

The resistivity was measured over the range of temperature from 293k to 473k using sensitive digital electrometer type keithley (616). The resistivity (ρ) of the films is calculated using the following equation:

$$\sigma_{d.c} = \frac{1}{\rho} = \frac{L}{R.A} \quad (2)$$

Where R is the resistance of sample, A the cross section area of the films and L is the distance between the electrodes.

In this model the area A = thickness of films (200 nm) × width of electrode (0.2 cm).

The activation energies could be calculated from the plot of lnσ versus 1000/T according to equation

$$\sigma = \sigma_{\circ} \exp\left(-\frac{E_a}{K_B T}\right) \quad (3)$$

Where σo is the minimum electrical conductivity at 0K, Ea is the activation energy which corresponds to ($E_g/2$) for intrinsic conduction, T is the temperature and kB is the Boltzmann's constant [21].

The hall coefficient (R_H) is determined by measuring the Hall voltage that generates the Hall field across the sample of thickness (t), by [22]:

$$R_H = \frac{V_H}{I} \cdot \frac{t}{B} \quad (4)$$

Where I is the current in (Amp.) passing through the sample, t is the thickness of the film in cm and B is the magnetic field strength

The n_H and R_H was calculated using the relation [23].

$$n_H = \frac{-1}{qR_H} \quad (5)$$

Hall's mobility (μ_H) can be written in the form [24]

$$\mu_H = \frac{\sigma}{n \cdot q} \quad (6)$$

Where q is the charge of electron and μH is Hall mobility measured with (cm2/V.s).

3. Characterization of thin films

The XRD analysis was employing in order to obtain the crystal quality and phase structure of the films. The electrical properties such as Dc conductivity and Hall measurements were study for $(TiO_2)_{1-x}(CdO)_x$ thin films.

4. Results and Discussion

4.1 Structural Properties

The crystalline structure of $(TiO_2)_{1-x}(CdO)_x$ recognized by study the phase of XRD for that material. Figure (2-a, b, c) shows the XRD patterns obtained for $(TiO_2)_{1-x}(CdO)_x$ thin films deposited on a glass substrate with thickness about 200 nm by pulse laser deposition method at different concentration of CdO x= (0.0, 0.05, 0.1, 0.15, 0.2) Wt. % prepare at RT and annealed to different annealing temperatures (423 and 523) K, respectively. According to International Centre for Diffraction Data (**ICDD**) cards, the structure of thin films showed a polycrystalline tetragonal structure for TiO_2 with Rutile phase classification. From Fig. (2), it is observed that the preferred orientation was along (110) direction for Rutile phase. Also, it is cleared from the x-ray patterns, which the peaks intensities increase with increasing of the doping ratio from 5 to 20%. It was noticed that the all films quality was improved with the increasing of annealing temperature, and observed new peak at concentration (0.15 and 0.2) Wt. %. The new Peak is belong to from CdO phase which is corresponding to reflection plane of (111).

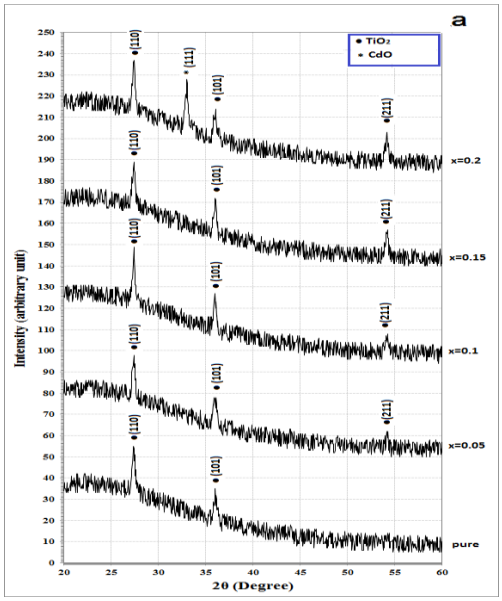

Figure 2-a: show the X-Ray diffraction for $(TiO_2)_{1-x}(CdO)_x$ thin films at RT

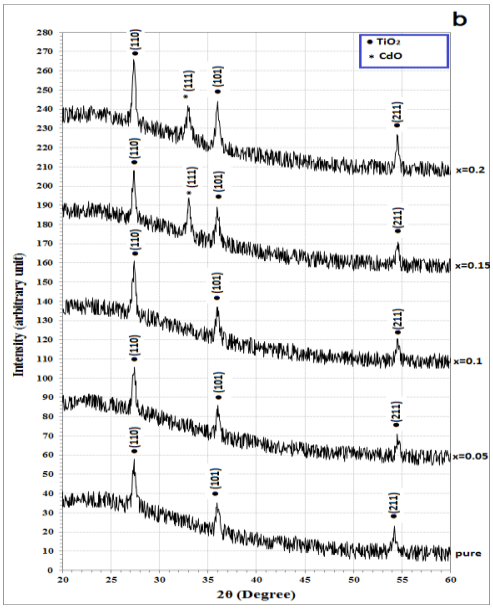

Figure 2-b: show the X-Ray diffraction for $(TiO_2)_{1-x}(CdO)_x$ thin films at annealing 423K.

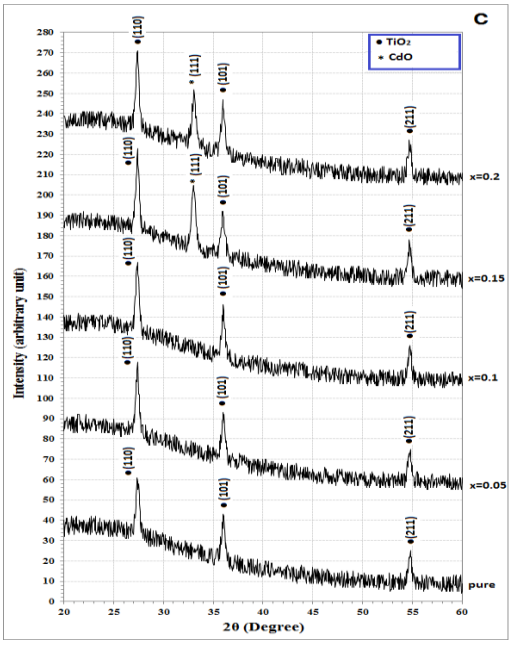

Figure 2-c: show the X-Ray diffraction for $(TiO_2)_{1-x}(CdO)_x$ thin films at annealing 523K

Table (1) gives the interplaner distance d, FWHM (Deg.), and grain size for the prepared samples in comparison with the standard value as in ICDD card. The structure of the $(TiO_2)_{1-x}(CdO)_x$ films has been investigated using XRD to ensure the stoichiometry of our material. We can observe that the values of d and 2θ are nearly similar to that in the ICDD cards as listed in Table (1). The average crystallite size, D, of thin film calculated using the Scherer's equation [25]:

$$D = k\lambda / \beta \cos\theta \qquad (7)$$

Where λ is the X-ray wavelength in nanometer (nm), β is the peak width of the diffraction peak profile at half maximum height resulting from small crystallite size in radians and K is a constant related to crystallite shape, normally taken as 0.9. The values of D are tabulated in table (1). It is cleared from the table that dhkl and average crystallite size increases with increasing of concentration of x. This implies that Cd partially substituted for Ti in TiO_2 structure.

Table 1: shows the peaks and its Bragg's angle, interplanar distance, and full width half at maximum and grain size for $(TiO_2)_{1-x}(CdO)_x$ thin films at different annealing and different concentration of CdO

Ts	2θ	FWHM	Int	dhkl	G.S	d_{hkl}	hkl
RT	27.35	0.4139	26.63	3.2582	20	3.2548	(110)
	33.05	0.3402	27.75	2.7081	24	2.7108	(111)
	36	0.4442	10.37	2.4927	19	2.4932	(101)
	54.2	0.4503	17.66	1.6909	20	1.6911	(211)
423	27.1	0.3389	31.09	3.2878	24	3.2548	(110)
	33.05	0.2994	16.32	2.7082	28	2.7108	(111)
	36.05	0.2949	18.74	2.4894	28	2.4932	(101)
	55.6	0.4476	14.55	1.6516	20	1.6911	(211)
523	27.65	0.2954	33.31	3.22359	28	3.2548	(110)
	33.1	0.2212	17.47	2.704212	37	2.7108	(111)
	35.25	0.2097	26.11	2.544043	40	2.4932	(101)
	54.25	0.4425	14.04	1.689502	20	1.6911	(211)

4.2 The Electrical Properties

The electrical properties of a $(TiO_2)_{1-x}(CdO)_x$ thin films deposited on glass substrate for different concentration of CdO at room temperature and annealed to different annealing temperatures will be presented. These properties include the D.C conductivity and the Hall Effect which gives information about the type, density and mobility of carriers.

4.3 DC Conductivity

Figure (3 - a, b, c) shows the variation of $\ln\sigma_{d.c}$ versus 1000/T for $(TiO_2)_{1-x}(CdO)_x$ film deposited by pluses laser on glass substrates with different concentration of CdO x= (0.0, 0.05, 0.1, 0.15, 0.2) Wt. % at room temperature and different annealing temperatures (423 and 523) k , with average thickness of (200) nm. From this figure, it is found that there are two stages of d.c conductivity mechanism throughout the temperatures range (293-473K). The first activation energy (Ea1) occurs at higher temperature within range (383-473) K and this activation energy is due to conduction of the carrier excited into the extended states beyond the mobility edge, while the second activation energy (Ea2) occurs at low temperature within range (293-383) K and the conduction mechanism of this stage is due to carrier's transport to localized states near the valence and conduction bands. It is cleared that the D.C. conductivity increases while the values of Ea1 and Ea2 decrease with the increasing of CdO as shown in Fig. (4) and table (2). However, with slight change in annealing temperature leads to increase in the activation energy which saturates the dangling bonds, i.e. there is reduction in the density of state which occurs at Fermi level that caused transferring the carriers from conductivity near Fermi level to the thermal activation conductivity at band gap.

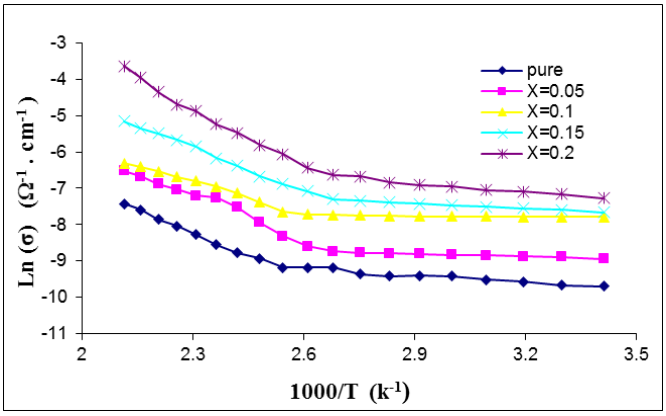

Figure 3-a: The relation between Ln (σ) versus reciprocal of temperature (1000/T) $(TiO_2)_{1-x}(CdO)_x$ films with different concentration of CdO at RT.

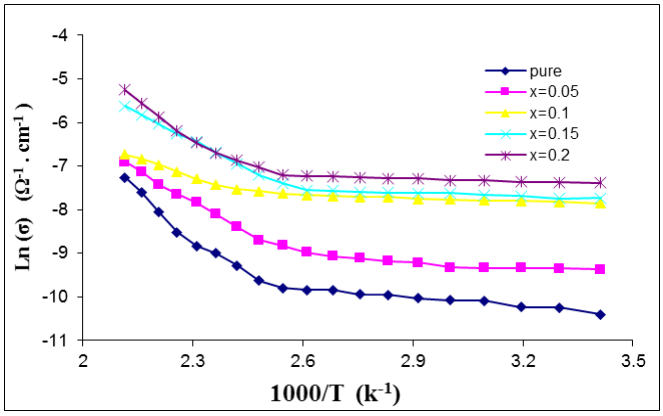

Figure 3-b: The relation between Ln (σ) versus reciprocal of temperature (1000/T) $(TiO_2)_{1-x}(CdO)_x$ films with different concentration of CdO at Ta= 423K

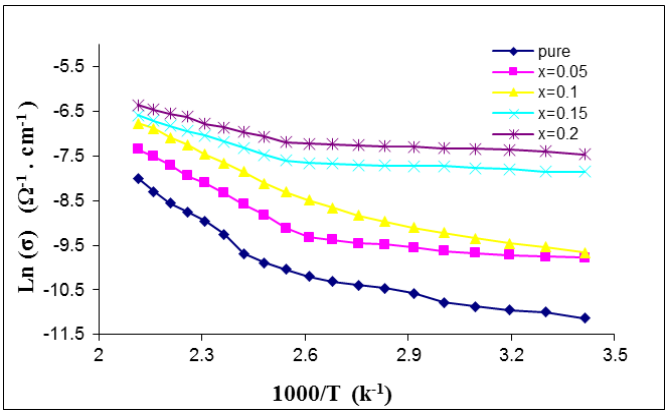

Figure 3-c: The relation between Ln (σ) versus reciprocal of temperature (1000/T) $(TiO_2)_{1-x}(CdO)_x$ films with different concentration of CdO at Ta= 523K

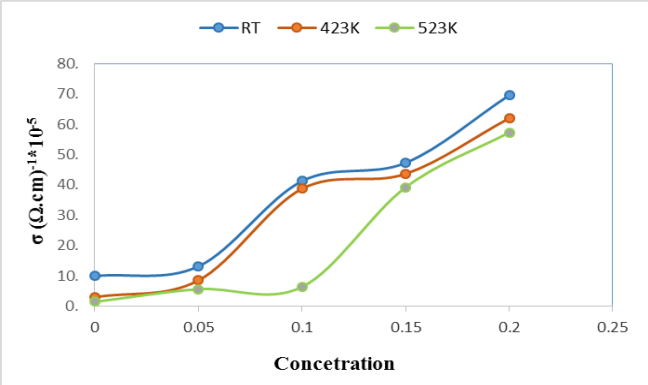

Figure 4: Variation of conductivity with concentration at different annealing temperature for $(TiO_2)_{1-x}(CdO)_x$ films

Table 2: Represents the values of conductivity, Ea1 and Ea2 and these ranges for $(TiO_2)_{1-x}(CdO)_x$ films with different concentration of CdO and different annealing temperatures.

Ts (K)	x%	**Ea1**(ev) at Range(298-383)k	**Ea2**(ev) at Range(383-473)k	σ (Ω^{-1}. cm^{-1})
RT	0	0.055	0.387	9.99E-05
	0.05	0.024	0.385	1.32E-04
	0.1	0.023	0.359	4.13E-04
	0.15	0.033	0.354	4.73E-04
	0.2	0.043	0.339	6.96E-04
423	0	0.061	0.431	3.03E-05
	0.05	0.048	0.394	8.54E-05
	0.1	0.029	0.366	3.87E-04
	0.15	0.029	0.355	4.36E-04
	0.2	0.026	0.343	6.20E-04
523	0	0.102	0.509	1.46E-05
	0.05	0.084	0.444	5.65E-05
	0.1	0.080	0.397	6.39E-05
	0.15	0.034	0.208	3.92E-04
	0.2	0.032	0.140	5.73E-04

4.5 Hall Effect

The type of charge carrier concentration (n_H) and Hall mobility (μ_H), have been estimated from Hall measurements. Table (3) illustrates the main parameters estimated from Hall Effect measurements for $(TiO_2)_{1-x(}CdO)_x$ films with different concentration of CdO at room temperature and annealed to (423 and 523) K, respectively. It is clear from this table that the all samples have a negative Hall coefficient (n-type), i.e. Hall voltage decreases with increasing of the current. Figure (5) and (6) show carriers concentration (n_H) and Hall mobility (μ_H) as a function of concentration and different annealing temperature. It is clear that the carrier concentration n_H increases while the Hall mobility μ_H decreases with the increasing of CdO content .When the films were annealed lead to showed an opposite manner a decreasing in the n_H while increasing in the value μ_H, as shown in Table (3). Increases the density of charge carriers is essentially because of the lowering the potential barrier. While the decreasing of mobility is come from the inverse relation between μ_H and n_H.

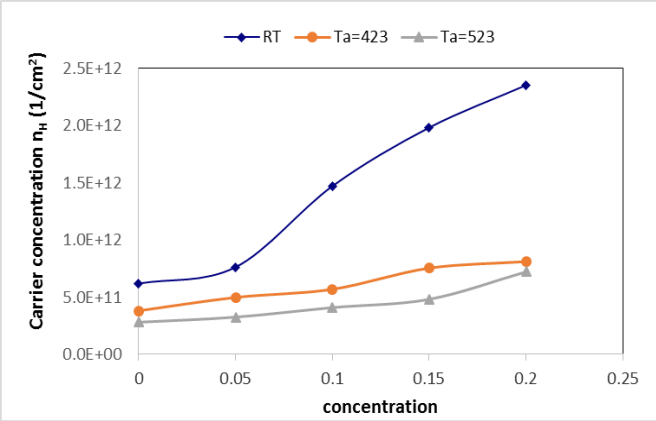

Figure 5: Show carriers concentration (n_H) as a function of CdO content at different annealing temperature for $(TiO_2)_{1-x}$ $(CdO)_x$ films

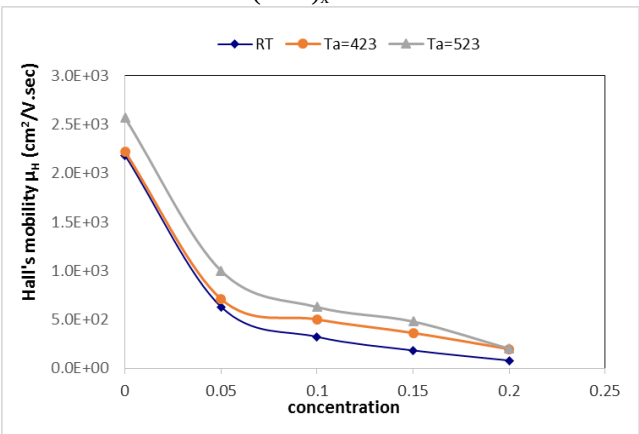

Figure 6: Show Hall mobility (μ_H) as a function of CdO content at different annealing temperature for $(TiO_2)_{1-x}$ $(CdO)_x$ films

Table 2: Represent the values of Hall coefficient, Conductivity, Hall mobility, Carrier concentration and type of concentration for $(TiO_2)_{1-x}(CdO)_x$ films with different concentration of CdO

Ts (K)	*X%*	R_H *10^6 (m^2/C)	μ_H*10^2 ($cm^2/V.sec$)	n_H*10^{11} ($1/cm^2$)	*type*
RT	0	10.10	21.82	6.188	n-type
	0.05	8.210	6.300	7.613	n-type
	0.1	4.256	3.222	14.69	n-type
	0.15	3.157	1.83	19.80	n-type
	0.2	2.660	0.8	23.50	n-type
423	0	16.43	22.19	3.804	n-type
	0.05	12.57	7.1	4.972	n-type
	0.1	11.0	5.0	5.682	n-type
	0.15	8.300	3.623	7.53	n-type
	0.2	7.715	1.970	8.101	n-type
523	0	22.28	25.65	2.805	n-type
	0.05	19.22	9.987	3.252	n-type
	0.1	15.30	6.272	4.085	n-type
	0.15	13.0	4.786	4.808	n-type
	0.2	8.673	2.0	7.206	n-type

5. Conclusion

In this paper, we have successfully synthesized the Rutile phase TiO_2 doped with CdO by PLD technique on glass substrates with different concentration at RT and different annealing (423 and 523)K. The results of XRD show that the films were polycrystalline with tetragonal structure. It was noticed that the all films quality was improved with the increasing of annealing temperature, and observed new peak at concentration (0.15 and 0.2) Wt. %. The new Peak is belong to from CdO phase which is corresponding to reflection plane of (111). The analysis of the d.c. conductivity illustrated that there are two stages of d.c conductivity mechanism throughout the temperature range (293-473K) that decreases while conductivity increases with increasing of the concentration of CdO. Hall Effect measurements show that all films have n- type charge carriers, and the concentration and annealing increase carriers concentration while the mobility decreases.

References

[1] S.Perumal, K.MonikandaPrabu, C.Gnana Sambandam and A. Peer Mohamed, "Synthesis and Characterization Studies of Solvothermally Synthesized Undoped and Ag-Doped TiO2 Nanoparticles Using Toluene as a Solvent," Journal of Engineering Research and Applications, vol. 4, no. 7, pp. 184-187, 2014.

[2] A. Fujishima, X. Zhang and D.A. Tryk, "TiO2 Photocatalysis and Related Surface Phenomena," Surf. Sci. Rep, vol. 63, no. 12, p. 512, 2008.

[3] Sillanpaa, K. Pirakanniemi and M., "Heterogeneous water phase catalysis as an environmental application: a," Chemosphere, vol. 48, pp. 1047-1060, 2002.

[4] B. Cojocaru, S ¸. Neat ¸u, E. Sacaliuc-Parvulescu, F. L ˆ evy, V.I. Parvulescu, and H. Garcia, "Influence of gold particle size on the photocatalytic activity for acetone oxidation of Au/TiO2 catalysts prepared by dc-magnetron sputtering," Applied Catalysis B, vol. 107, p. 140–149, 2011.

[5] D. Y. Chen, C. C. Tsao, and C. Y. Hsu, "Photocatalytic TiO2 thin films deposited on flexible substrates by radio frequency (RF) reactive magnetron sputtering," Current Applied Physics, vol. 12, p. 179–183, 2012.

[6] A. M. More, T. P. Gujar, J. L. Gunjakar, C. D. Lokhande, and S.Joo, "Growth of TiO2 nanorods by chemical bath deposition," Applied Surface Science, vol. 255, p. 2682–2687, 2008.

[7] H. Zhu, J. Yang, S. Feng, M. Liu, J. Zhang, and G. Li, "Growthof TiO2 nanosheet-array thin films by quick chemical bath deposition for dye-sensitized solar cells," Applied Physics, vol. 105, p. 769–774, 2011.

[8] J. K. Yao, H. Y. Li, Z.and X. Fan, "Comparison of TiO2 and ZrO2 films deposited by electron-beam evaporation and by sol-gel process," Chinese Physics Letters, vol. 24, no. 4, p. 1964–1966, 2007.

[9] O. Duyar, F. Placido, and H. Zafer Durusoy, "Optimization of TiO2 films prepared by reactive electron beam evaporation of Ti3O5," Journal of Physics, vol. 41, no. 9, 2008.

[10] J. C. Yu, W. Ho, J. Yu, S. K. Hark, and K. Iu, "Effects of tri fluoroacetic acid modification on the surface microstructures and photocatalytic activity of mesoporous TiO2 thin films," Langmuir, vol. 19, p. 3889–3896, 2003.

[11] S. Zhan, D. Chen, X. Jiao, and C. Tao, "Long TiO2 hollow fibers with mesoporous walls: sol-gel combined electrospun fabrication and photocatalytic properties," Journal of Physical Chemistry B, vol. 110, no. 23, p. 11199–11204, 2006.
[12] J. Zhu, F. Chen, J. Zhang, H. Chen, and M. Anpo,, "“Fe3+-TiO2 photocatalysts prepared by combining sol-gel method with hydrothermal treatment and their characterization," Journal of hydrothermal treatment and their characterization, vol. 180, no. 1-2, pp. 196-204, 2006.
[13] N. Arconada, A. Duran, S. Su ´ arez et al, "Synthesis and phopocatalytic properties of dense and porous TiO2-anatase thin films prepared by sol-gel," Topics in Catalysis, vol. 86, no. 1-2, pp. 1-7, 2009.
[14] Z. Luo, H. Cai, X. Ren, J. Liu, W. Hong, and P. Zhang, "Hydrophilicity of titanium oxide coatings with the addition of silica," Materials Science and Engineering B, vol. 138, no. 2, p. 151–156, 2007.
[15] Turner, H. M. Smith and A. F., "Vacuum Deposited Thin Films Using a Ruby Laser," Appl., vol. 4, no. 1, p. 47, 1965.
[16] D. Dijkkamp, T. Venkatesan, X. D. Wu, S. A. Shareen, N. Jiswari, Y. H. Min-Lee, W. L., "Preparation of Y-Ba-Cu Oxide Superconductor Thin," Appl. Phys., vol. 51, p. 619, 1987.
[17] Rodriguez, R.Ferro and J. A., "Influence of F-doping on the transmittance and electron affinity of CdO thin films suitable for solar cells technology," Sol. Energy Mater. Sol. Cells, vol. 64, p. 363–370, 2000.
[18] T.K Subramanyam, S Uthanna and B Srinivasulu Naidu, "Preparation and characterization of CdO films deposited by dc magnetron reactive sputtering," Mater Lett, vol. 35, pp. 214-220, 1998.
[19] P. R. Patil, P. S. Patil and C. D. Lokhande, "Spray pyrolysis of WOx thin films," Indian Journal of Physics, vol. 14, p. 266, 1995.
[20] Kadhim A. Adem, Mohammed A. Hameed and Raied K. Jamal, "Study of Optical and Structures for TiO2 prepared by Pulse Laser Deposition," International Journal of Science and Technology, vol. 2, no. 12, pp. 886-890, 2013.
[21] R. Grenier, "Semiconductor Device," Electronic Energy Series,McGrawHill, Book Co.Inc, vol. 369, p. 198, 1961.
[22] D. A. Neaman, Semiconductor Physics and Devices, Boston: Basic Principles, Richard D. Irwin, Inc, 1992.
[23] S. M. Sze, Physics of Semiconductor Devices, 2nd ed ed., New York: John Wiley and Sons, Inc, 1981.
[24] C. Kittel, Introduction to Solid State Physics, 8th ed ed., New York: John Wiley and Sons Inc, 2005.
[25] Ahmad Monshi, Mohammad Reza Foroughi and Mohammad Reza Monshi, "Modified Scherrer Equation to Estimate More Accurately," World Journal of Nano Science and Engineering, vol. 2, pp. 154-160, 2012.

Author Profile

Ghuson H. Mohammed, is currently a professor of physics At the Applied physics center, Baghdad, Iraq. He received his Ph.D Degree from Heriot -Watt University (U.K) in 1990. His currently research Interests include the preparation of nano films (semiconductors and polymers) by different methods for applications of gas sensors, solar cells and optical detectors. He has written 40 scientific publications in this area.

Ahmed M. Savory, M.SC student in physics department, college of science, Baghdad University. His research interest includes the preparation of thin films and applications.